Revista Mexicana de Astronomía y Astrofísica, **28**, 173-180 (1994)

MOLECULAR SHOCKS IN HERBIG-HARO 1

A. Noriega-Crespo

Infrared Processing and Analysis Center, Caltech, and
Maria Mitchell Observatory

and

P.M. Garnavich

Dominion Astrophysical Observatory
Herzberg Institute of Astrophysics

Received 1994 May 10

RESUMEN

Se presentan observaciones espectroscópicas de baja resolución en el infrarrojo (1.2−2.4 μm) alrededor de dos condensaciones (A & G) de la superficie de trabajo del objeto Herbig-Haro 1, para estudiar la naturaleza de sus choques moleculares. Encontramos que el espectro de la condensación A, además de las líneas intensas a (1,0) S(1) 2.121 μm y (2,1) S(1) 2.247 μm, tiene varias líneas de hidrógeno molecular, como también de [Fe II] 1.257 μm y [Fe II] 1.644 μm. La condensación G no muestra H_2 pero tiene líneas de [Fe II] igualmente intensas que A. Comparamos las columnas de densidad de H_2 de HH1-A con las predichas por los modelos de choque de clase C y J. Es difícil de distinguir entre estos modelos dadas nuestras observaciones. Medimos, a través de las líneas de [Fe II], una extinción de $A_V = 6.7 \pm 1.4$ magnitudes (es decir un $E(B-V) \sim 2.2 \pm 0.4$ magnitudes), que es más grande de lo que se obtiene de las líneas de [S II].

ABSTRACT

We present low resolution, infrared spectroscopic observations (1.2−2.4 μm) near two optical condensations (A & G) of the leading working surface of Herbig-Haro object 1, in order to study the nature of their molecular shocks. Condensation A spectra show several molecular hydrogen lines, besides the strong (1,0) S(1) 2.121 μm and (2,1) S(1) 2.247 μm lines, as well as [Fe II] 1.257 μm and [Fe II] 1.644 μm. Condensation G does not show H_2 lines, but its [Fe II] lines are as strong as those in A. We compare the H_2 column densities of HH1-A, with those predicted by J-type and C-type shock models. It is difficult to distinguish between these models given our observations. From the [Fe II] lines we estimate an extinction of $A_V = 6.7 \pm 1.4$ magnitudes (or an $E(B-V)$ of 2.2 ± 0.4 magnitudes), which it is higher than what it is obtained from the [S II] lines measurements.

Key words: **ISM – JETS AND OUTFLOWS — ISM – MOLECULES — SHOCK WAVES**

1. INTRODUCTION

Herbig-Haro (HH) objects and jets are spectacular tracers of the ubiquitous phenomenon of mass outflow during the formation of protostellar objects (see e.g., Shu, Adams, & Lizano 1987). Collimated bipolar stellar-disk wind models account for most of the general properties of these objects (see e.g., reviews by Pudritz, Pelletier, & Gomez de Castro 1991; Reipurth 1991; Edwards, Ray, & Mundt 1993; Raga 1993; Raymond et al. 1994). Since the realization that most of the emitted light from HH objects arises in the recombination regions behind shock waves (Schwartz 1975), a considerable effort has been invested in comparing spectroscopical observations with the emitted spectra predicted by shock models (Dopita 1978; Raymond 1979; Hartigan, Raymond, & Hartmann 1987). At low shock velocities, $\leq$ 50 km s^{-1}, it is found that an important fraction of the total emission is released at infrared wavelengths from molecular rotational-vibrational transitions of H_2, CO and H_2O, as well as from atomic and ionic fine structure (mostly forbidden) transitions, e.g., [Fe II] 1.64 μm, [O I] 63 μm, [C II] 157 μm and [Si II] 35 μm (see e.g., Hollenbach & McKee 1979).

Low velocity shocks ($\leq$ 50 km s^{-1}) in molecular

material have been studied for some time (see e.g., the excellent review by Draine & McKee 1993) and broadly speaking can be separated into two types (Draine 1980; Chernoff 1987): J-shocks and C-shocks. In a J-type shock, like in an atomic shock, there is a discontinuous change in the density, temperature and velocity across the front. The magnetic fields and ionization fractions associated with them are relatively small ($\sim 100\ \mu$G), and large ($\geq 10^{-5}\ \mu$G), respectively. In a C-type shock stronger magnetic fields and lower ionization fractions are involved. Under these conditions the ion and the neutral matter in the molecular material react differently to a disturbance. Ionmagnetosonic waves, essentially, prepare the neutral fluid ahead the shock (through ambipolar diffusion) so when it arrives changes in density, temperature and velocity are continuous. In the case of H_2, for instance, C-shocks allow for higher shock velocities (~ 50 km s^{-1}) without dissociating the molecules.

In this paper we present low resolution NIR (1.2 – 2.4 μm) observations of emission near the optical condensations HH1-A and HH1-G, which are downstream structures of the bowshock-like working surface of HH1. We selected this region based on our H_2 (1,0) S(1) 2.12 μm imaging study

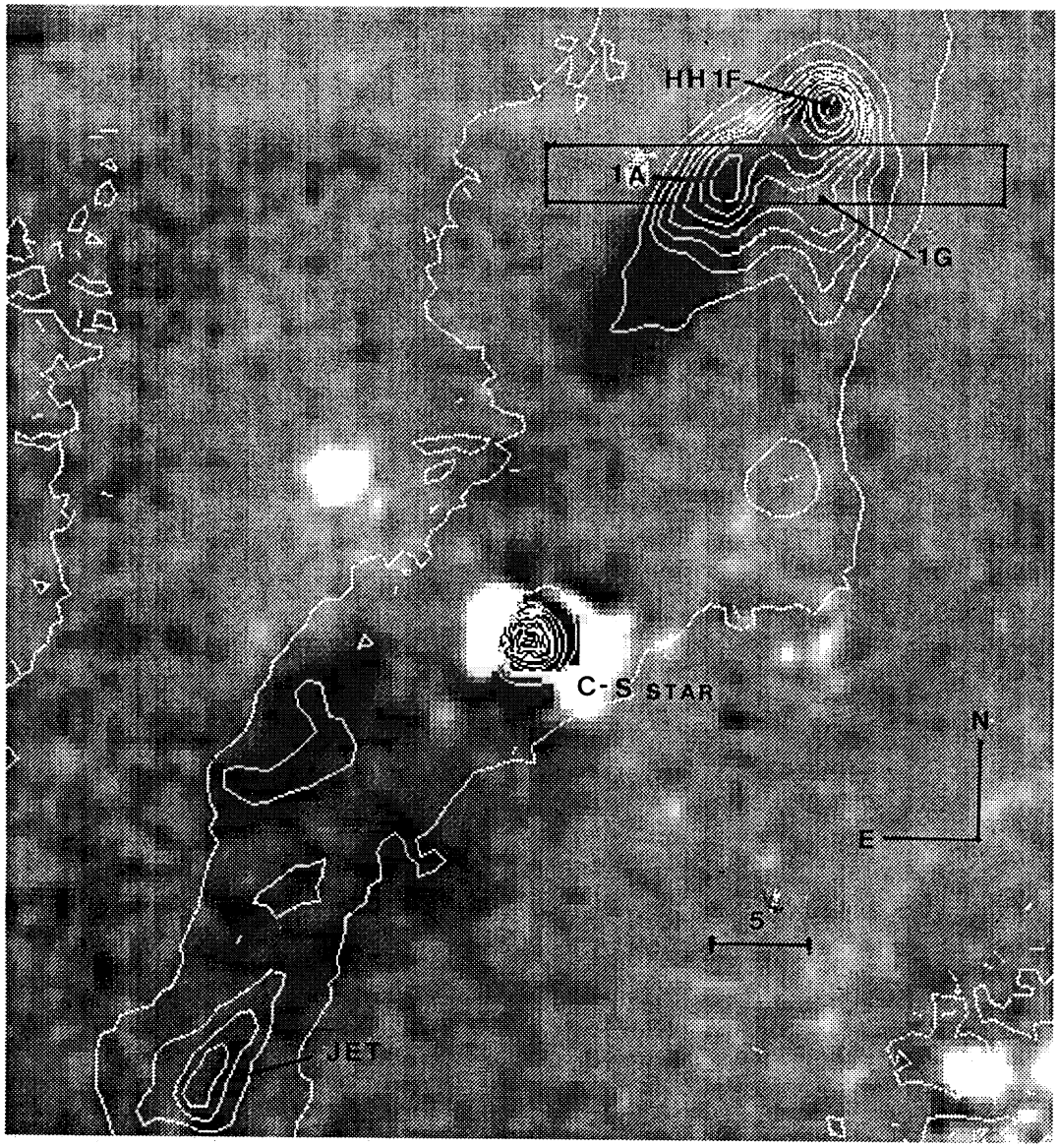

Fig. 1. Near infrared image of the HH1 region in the 1 – 0 S(1) 2.121 μm emission line (Noriega-Crespo & Garnavich 1994). The linear contour lines correspond to the [S II] 6717/31 A emission. The field is $\sim 1.'0$ and the approximately position of the slit is depicted.

TABLE 1

SPECTRAL LINE FLUXES[a] AND COLUMN DENSITIES

$\lambda(\mu m)$	Identification	HH1-A	HH1-G[b]	$E(v'J')$(K)	$\ln N(v'J')/g$
1.257	[Fe II]	7.9	8.0	...	...
1.294	[Fe II]	2.0	...	...	...
1.321	[Fe II]	3.7	4.0	...	...
1.533	[Fe II]	1.8	0.7	...	...
1.644	[Fe II]	12.0	12.0	...	...
1.687	H_2 (1,0) S(9)	0.9	...	15735	10.4
1.714	H_2 (1,0) S(8)	2.9	...	14233	12.5
1.732	?	0.9	...	...	...
1.747	H_2 (1,0) S(7)	5.7	...	12828	11.9
1.760	?	1.5	...	...	...
1.788	H_2 (1,0) S(6)	3.6	...	11521	12.5
2.033	H_2 (1,0) S(2)	7.6	...	7584	14.0
2.072	H_2 (1,0) S(3)	3.0	...	13902	11.4
2.121	H_2 (1,0) S(1)	18.0	...	6957	14.1
2.154	H_2 (2,1) S(2)	1.5	...	13162	12.0
2.201	H_2 (3,2) S(3)	1.5	...	19102	10.8
2.222	H_2 (1,0) S(0)	7.6	...	6477	15.1
2.247	H_2 (2,1) S(1)	4.3	...	12561	12.4
2.406	H_2 (1,0) Q(1)	2.7	...	6155	13.0

[a] Flux in 10^{-14} erg cm^{-2} s^{-1}.

[b] West of H_2 emission.

(Noriega-Crespo & Garnavich 1994) which shows a remarkable asymmetry in the emission from the two knots. The spectroscopic observations are shown in § 2. In § 3 we compare the H_2 observed column densities with those predicted by J-type and C-type plane parallel molecular shock models (Smith 1994b). We summarize our main results in § 4.

2. OBSERVATIONS

On 1994 January 30, spectra of HH1 were obtained with OSIRIS on the 1.5-m telescope at CTIO. OSIRIS was used in its cross-dispersed mode which allowed spectra in the *J*, *H* and *K* bands to be recorded simultaneously with a resolving power of 400. OSIRIS is designed so that the atmospheric absorption bands fall at the edges of the detector. In the cross-dispersed mode, the long-wavelength limit is determined by intersection of the spectrum and the edge of the detector (which depends on the position of the target along the slit). At the slit center, this limit is approximately 2.4 μm, and fluxes near this wavelength have a significant uncertainty. The 3″ wide slit was placed on the brightest H_2 emission knot which is close to optical emission knot HH1-A. The slit was oriented in the east-west direction, so emission near the optical knot HH1-G was also recorded (see Figure 1).

Three 600 second exposures of HH1 were alternated with exposures of blank sky 30″ to the north. The sky images were subtracted from the HH1 spectra and the results divided by a dome flat field. The frames were then median averaged. Spectra of δ Dor were obtained and used as a guide to extract the HH1 spectra as well as flux calibrate the data. Spectra corresponding to emission near HH1-A and HH1-G were extracted separately using a 5″ aperture (see Figure 2). Thus, the fluxes derived here are averaged from a 3″ × 5″ area of sky. The value obtained for the 1 – 0 S(1) 2.121 μm line for HH1-G (see Table 1), for instance, is within 5% of the flux obtained by Zealey et al. (1992) of 1.9×10^{-13} erg cm^{-2} s^{-1} for the HH1 "southeast"region using a 14 arcsec aperture. The errors in our fluxes are $\pm 0.4 \times 10^{-13}$ erg cm^{-2} s^{-1} for the bright lines and $\pm 0.6 \times 10^{-13}$ erg cm^{-2} s^{-1} for the weaker ones.

3. DISCUSSION

3.1. Comparison with the Models

The H_2 lines provide a unique opportunity to search for the signature of magnetic molecular shocks in star forming regions. As mentioned in the introduction, both C-type and J-type shocks are expected to be present depending on the pre-shock parameter space. In this section we present a comparison of our observations with published shock models relevant to Herbig-Haro objects. We first compare the intensity ratios with J-type shocks

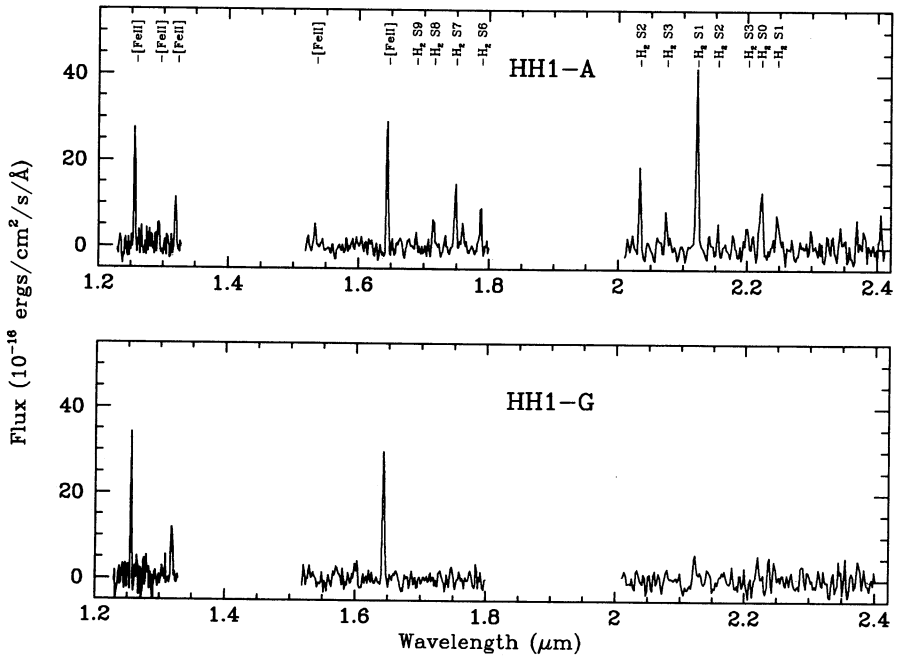

Fig. 2. NIR spectra of HH1-A and HH1-G (see Table 1).

with magnetics precursors, and later on we use the column density of the different upper H_2 levels and compare them with those predicted by C-type and J-type models.

3.2. *J-Shocks with a Magnetic Precursor*

A comparison of the observations with shock models should always be regarded merely as a guide of the pre-shock conditions, since in general, shocks cannot be described by a unique temperature, density and ionization fraction. A first approximation consists in comparing the observed line ratios with those predicted by plane parallel shock models. Using the measured intensities (Table 1), we compare them with those predicted by J-type models with magnetic precursors calculated by Curiel (1992) for different preshock densities and magnetic fields (see Table 2). The models have the same initial ionization fraction (10^{-5}) and chemical composition. Molecular shocks depend on the CO, CH, OH and H_2O abundances, besides the atomic species (for details see (Curiel 1992)). The equivalent velocity V_{eq} in Table 2, refers to the net shock velocity moving into the molecular material, which is equivalent to V_s in the neutral matter (McKee & Hollenbach 1987).

We conclude from Table 2, that the models cover the observed range of intensity ratios, however, the selected models systematically overestimate the 2.41 μm to 2.12 μm ratio (however, the 2.41 μm line falls at the egde of the detector and its flux is rather uncertain). Perhaps the best agreement is for the relatively fast shock model (m7) with $V_s = 100$ km s^{-1} and $N_H = 600$ cm^{-3}. Although these values are very close to what was determined for HH1 from optical emission lines (Solf, Böhm, & Raga 1988), they refer to the preshock conditions ahead of the apex of a 'bowshock' (Noriega-Crespo, Böhm, & Raga 1989), and not necessarily farther 'downstream', where the H_2 emission originates.

3.3. *C-type and J-type Shocks*

The H_2 emission lines can be compared in a slightly more sophisticated way, which involves the determination of the column densities at each energy upper level. Using a Boltzmann factor for the population levels it is possible to determine either one excitation temperature or several excitation temperatures (or shock velocities) depending if one assumes a global thermal equilibrium (Gredel, Reipurth, & Heathcote 1992) or a local equilibrium between the levels (Smith 1994b). We have considered both approximations. In the first case (following Gredel et al. 1992), the intensities for the vibrational (v') and rotational (J') upper level are transformed into column densities by using:

$$I(v'J') = \frac{hc}{4\pi}\tilde{\nu}A(v'J')N(v'J') \quad , \qquad (1)$$

TABLE 2

J-SHOCK MODELS[a,b]

Parameter	m1	m2	m3	m4	m5	m6	m7	Data
V_s (km s^{-1})	30	55	17	50	50	50	100	...
n_H (cm^{-3})	10^3	10^3	10^4	10^3	300	300	600	...
B_0 (μG)	70	70	70	117	110	11	70	...
V_{eq} (km s^{-1})	43	61	42	64	80	58	105	...
2.04 μm	0.39	0.83	0.42	0.35	0.63	0.34	0.39	0.42
2.12 μm	1.00	1.00	1.00	1.00	1.00	1.00	1.00	1.00
2.22 μm	0.27	0.30	0.23	0.32	0.56	0.29	0.30	0.42
2.25 μm	0.49	0.24	0.38	0.30	0.34	0.27	0.23	0.24
2.41 μm	0.91	0.92	0.73	0.97	1.18	0.91	0.86	0.15
F(2.12 μm)[c]	5.4	8.0	55.0	32.0	37.0	2.1	25.0	18.0

[a] Shock models from Curiel (1992).
[b] In all cases, $X_e(10^{-5}) = 1.0$.
[c] Flux in 10^{-14} erg cm^{-2} s^{-1}, for r $\sim$ 2.″5 and d = 460 pc.

where $N(v'J')$ is the column density, $\tilde{\nu}$ is the wavenumber (Dabrowski 1984) and $A(v'J')$ is the transition probability (Turner, Kirby-Docken, & Dalgarno 1977). For a global thermalization, the populations are related by a Boltzmann factor, i.e.,

$$N(v'J') \propto g e^{(-E(v'J')/kT_{ex})} , \qquad (2)$$

where $E(v'J')$ is the excitation energy, g the statistical weight and T_{ex} the excitation temperature. Clearly, T_{ex} can be derived from the slope of the linear relation between ln $N(v'J')/g$ and $E(v'J')/k$. The values obtained by this exercise are presented in Table 1, and in Figure 3 we show ln $N(v'J')/g$ versus $E(v'J')/k$. The solid line is a least-squares fit which corresponds to T_{ex} = 3344 $\pm$ 540 K. The $\sim$ 16% uncertainty in the excitation temperature already indicates that there are relatively large fluctuations in the populations. Indeed from the data it seems that column densities from nearby vibrational levels (i.e., close by in energy) define different temperatures around the mean excitation temperature (see Fig. 3), as expected in a shock with a more complex thermal structure (Curiel, private communication). This suggests that perhaps a 'local thermal equilibrium' is a more appropriate approximation. Such analysis has been successfully carried for the HH 90/91 outflow by Smith (1994b), using C-type and J-type shocks. The H_2 intensities and column densities determined in HH 91/90 (Gredel et al. 1992) are not far from those of HH1-A, and therefore we have taken similar models (Smith 1994b) to interpret our observations. The

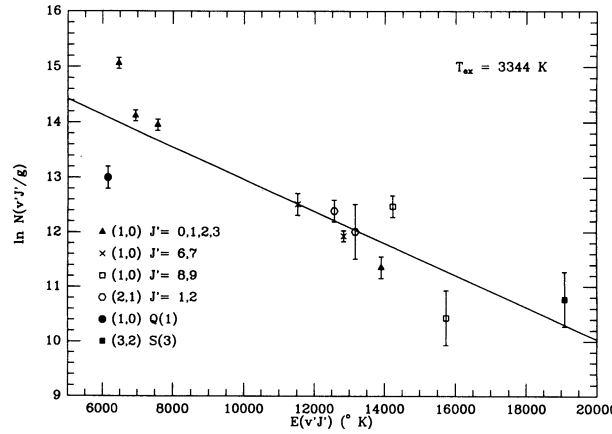

Fig. 3. H_2 excitation diagram for HH1-A. The straight line is a least-squares fit to the data and corresponds to $T_{ex} \sim$ 3344 K.

models depend in detail of various parameters (see e.g., Smith & Brand 1990; Smith, Brand, & Moorhouse 1991; Smith 1994a), some of these worth notice are: the initial preshock density (3×10^5 cm^{-3}); ionization fraction per hydrogen atom (10^{-5} for J-shocks, and 10^{-7} for C-shocks); an Alfven velocity (for C-shocks, of V_A = 2 km s^{-1}, which implies a magnetic field $\sim$ 600 μG), with the magnetic field parallel to the shock (Smith 1994b).

In Figure 4, we show the comparison between our measurements and the shock models. For dis-

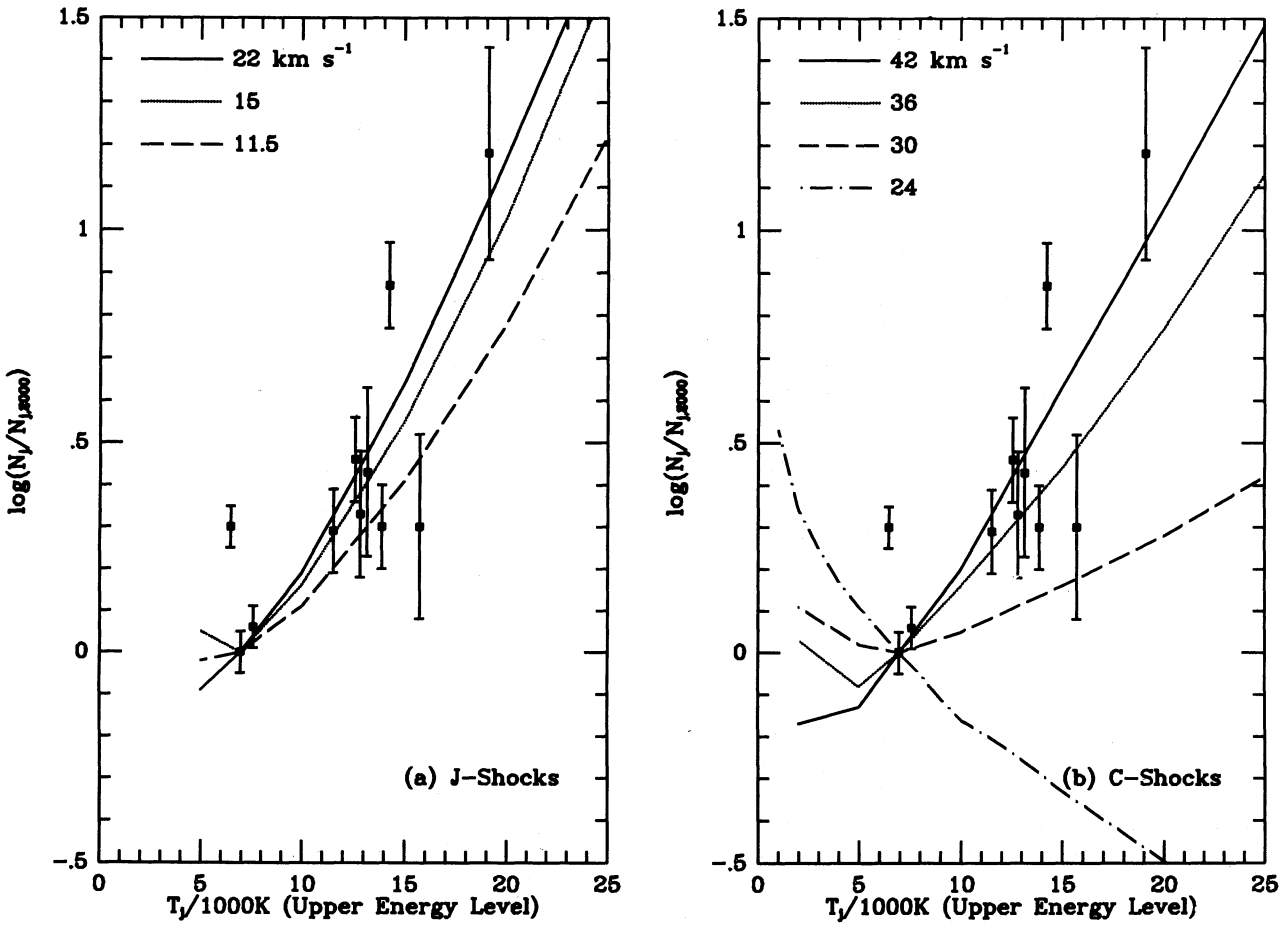

Fig. 4. The normalized H_2 column densities for different lines as a function of their upper level energy are compared with molecular J and C shock models (following Smith 1994b).

play the column densities have been normalized (Smith 1994b) first by dividing them by a factor $\exp(-T_j/2000\ \mathrm{K})$ where T_j is the upper temperature (energy) for level j, and then with respect to the 1−0 S(1) 2.121 μm column density.

At a glance J and C type shock models seem to do an adequated job in explaining the observations (see Fig. 3). J-type shocks velocities of 11 through 22 km s^{-1} are "equivalent" to C-type shocks of 30 through 42 km s^{-1}. There are few data points for which the models do not fare well, the relatively bright (1,0) S(0) 2.222 μm, the weak (1,0) S(9) 1.687 μm and the intermediate intensity (1,0) Q(1) 2.406 μm. This last one (outside the plot range, with a value $\log(N/N_{j,2000} \sim -0.66$) is at the edge of the detector and its intensity may have been underestimated.

Unlike the case for HH 90/91, where the J-type models seem to match better the observations (Smith 1994b), in HH1-A the relatively scatter of some of the points does not really permit us to distinguish between C-type and J-type shocks.

3.4. The [Fe II] Lines

Besides the H_2 lines some strong [Fe II] are observed (see Figure 2 and Table 1) in HH1-A and HH1-G. Particularly useful are the bright [Fe II] lines at 1.26 μm and 1.65 μm, which have a common upper level, and can be used to estimate the absorption along the line of sight to the [Fe II] emission region. The [Fe II] lines are equally bright in condensations 1-A and 1-G, which already indicates that at least their asymmetry in their H_2 emission is not due to extinction.

The observed ratio for [Fe II] 1.26 μm to [Fe II] 1.65 μm is 0.7 ± 0.1 while the predicted value is 1.36 (Nussbaumer & Storey 1988; Oliva, Moorwood, & Danziger 1989, 1990). Using the IR extinction law

derived by Rieke & Lebofsky (1985), the observed ratio is equivalent to 6.7 ± 1.4 magnitudes of visual extinction or an *E(B-V)* of 2.2 ± 0.4 magnitudes. This latter value is ~ 5 times larger that what it has been estimated optically using the [S II] *auroral* (4068, 4072 A) to *transauroral* (10318, 10336, 10370 A) line ratios, which give an average value *E(B-V)* = 0.43 ± 0.04 (Solf, Böhm, & Raga 1988).

It is difficult to understand this discrepancy based on the standard ISM extinction and/or θ Orioni curves (Mathis 1990), since both curves are identical for $\lambda > 0.7$ μm. Differences in the extinction also arise when analyzing the interstellar reddening at optical and ultraviolet wavelengths (Böhm, Raga, & Binette 1991), and these disparities suggest drastic changes in the dust environment around HH1. A contributing effect may be the differing absorption between the NIR and the optical which results in a greater path length for absorption in the infrared.

4. CONCLUSIONS

We present near infrared (1.2 – 2.4 μm) low resolution spectroscopic observations near the HH1-G and HH1-A optical condensations ('downstream' of HH1), in order to understand the nature of the molecular shocks associated with working surfaces in Herbig-Haro objects. We selected HH1-A and G based on our H_2 (1,0) S(1) 2.121 μm images which display an asymmetry in their emission properties, i.e., 1-A is visible in H_2 while 1-G is not. This is relatively surprising given how close the HH1 working surface resembles a 'bowshock' (Noriega-Crespo et al. 1989), and therefore, similar emission is expected to arise from its 'wings' downstream.

We identified ~ 10 H_2 emission lines in HH1-A, including strong (1,0) S(1) 2.121 μm and (2,1) S(1) 2.247 μm, and ~ 5 [Fe II] lines in both HH1-A and G. We used the H_2 lines to obtain the corresponding column densities for their different upper energy level ($N(v'J')$), and derived their excitation temperatures. Under the assumption of a global thermal equilibrium for the entire shock structure, we found an excitation temperature of T_{ex} = 3344 ± 540 K. The relatively large fluctuations in the $N(v'J')$s lead us to assume a local thermal equilibrium instead, where individual excitation temperatures (or shock velocities) are derived, and we compared them with different molecular shock models. We found that from our data is difficult to distinguish between weakly magnetized J-type shocks with velocities ranging from ~ 11 – 22 km s^{-1}, or C-type shocks with fields of ~ 600 μG and velocities ranging from ~ 30 – 42 km s^{-1}.

We tried also a direct comparison of the H_2 intensity ratios (normalized to (1,0) S(1) 2.121 μm) with J-shock models with magnetic precursors, and although a fast shock (~ 100 km s^{-1}, B ~ 70 μG, n_H ~ 600 cm^{-3}) seems to match several of the ratios, its velocity is too high for that expected in those regions.

Finally, we used the [Fe II] 1.26 μm to [Fe II] 1.65 μm ratio to determine the extinction in both HH1-A and G. We found a visual extinction of *E(B-V)* = 2.2 ± 0.4 magnitudes, which is a factor ~ 5 higher than what it is measured by using the transauroral and auroral [S II] lines. This suggests variations in the dust environment around HH1, as well as differences in the optical depths for the NIR and [S II] emission.

It is a pleasure to thank S. Curiel, R. Gredel, and A. Raga for their enlightening ideas on molecular shocks, to R. Dgani-Knill and D. van Buren for useful conversations, and to M. Smith (the referee) for his comments and careful reading of manuscript. ANC research is supported by NASA Long Term Astrophysics Program (through IPAC), by the grants NSF-REU AST9300391 and the Perking Fund (through MMO). We also thank D. Depoy for advice on using the instrument and acknowledge NSF grants AST 90-16112 and AST 92-18449, which supported the construction of OSIRIS.

REFERENCES

Böhm, K.H., Raga, A.C., & Binette, L. 1991, PASP, 103, 85
Curiel, S. 1992, Ph.D. thesis, Universidad Nacional Autónoma de México
Chernoff, D.F. 1987, ApJ, 312, 143
Dabrowski, I. 1984, CanJPhys., 62, 1639
Dopita, M. 1978, ApJS, 37, 117
Draine, B.T. 1980, ApJ, 241, 1021
Draine, B.T., & Mckee, C.F. 1993, ARA&A, 31, 373
Edwards, S., Ray, T., & Mundt, R. 1993, in Protostars and Planets III, ed. E.H. Levy & J.I. Lunine (Tucson: The University of Arizona Press), 567
Gredel, R., Reipurth, B., & Heathcote, S., 1992, A&A, 266
Hartigan, P., Raymond, J., & Hartmann, L. 1987, ApJ, 316, 323
Hollenbach, D.J., & McKee, C.F. 1979, ApJS, 41, 555
Mathis, J.S. 1990, ARA&A, 28, 37
McKee, C.F., & Hollenbach, D.J. 1987, ApJ, 342, 306
Noriega-Crespo, A., Böhm, K.H., & Raga, A.C. 1989, AJ, 98, 1388
Noriega-Crespo, A., & Garnavich, P.M. 1994, AJ, in press
Nussbaumer, H., & Storey, P.J. 1988, A&A, 193, 327
Oliva, E., Moorwood, A.F.M., & Danziger, I.J. 1989, A&A, 214, 307
_____. 1990, A&A, 240, 453
Pudritz, R.E., Pelletier, G., & Gomez de Castro, A. 1991, in The Physics of Star Formation and Early Stellar Evolution, ed. Ch.J. Lada, & N.D. Kylafis (Dordrecht: Kluwer Academic Publishers), 539
Raga, A.C. 1993, Ap&SS, 208, 163
Raymond, J.C. 1979, ApJS, 39, 1
Raymond, J.C., Morse, J.A., Hartigan, P., Curiel, S., & Heathcote, S. 1994 in Stellar and Circumstellar

Astrophysics, ed. G. Wallerstein, & A. Noriega-Crespo, ASP Series 57, p. 53
Reipurth, B. 1991, in The Physics of Star Formation and Early Stellar Evolution, ed. Ch.J. Lada, & N.D. Kylafis (Dordrecht: Kluwer Academic Publishers), 497
Rieke, G.H., & Lebofsky, M.J. 1985, ApJ, 288, 618
Schwartz, R.D. 1975, ApJ, 195, 631
Shu, F.H., Adams, F.C., & Lizano, S. 1987, ARA&A, 25, 1
Smith, M.B., & Brand, P.W.J.L. 1990, MNRAS, 243, 498
Smith, M.B., Brand P.W.J.L, & Moorhouse, A. 1990, MNRAS, 248, 451
Smith, M.D. 1994a, MNRAS, 266, 238
_____. 1994b, A&A, in press, (preprint)
Solf, J., Böhm, K.H., & Raga, A.C. 1988, ApJ, 334, 229
Turner, J., Kirby-Docken, K., & Dalgarno, A. 1977, ApJS, 35, 281
Zealey, W.J., Williams, P.M., Sandell, G., Taylor, K.N.R., & Ray, T.P. 1992, A&A, 262, 570

Alberto Noriega-Crespo: Infrared Processing and Analysis Center, Caltech, Pasadena, CA 91125 U.S.A. E-mail: alberto@ipac.caltech.edu.
Peter M. Garnavich: Dominion Astrophysical Observatory, Herzberg Institute of Astrophysics, Victoria BC, V8X 4M6 Canada.